



# Lawrence Berkeley Laboratory

UNIVERSITY OF CALIFORNIA

## CHEMICAL BIODYNAMICS DIVISION

Submitted to The Journal of Chemical Physics

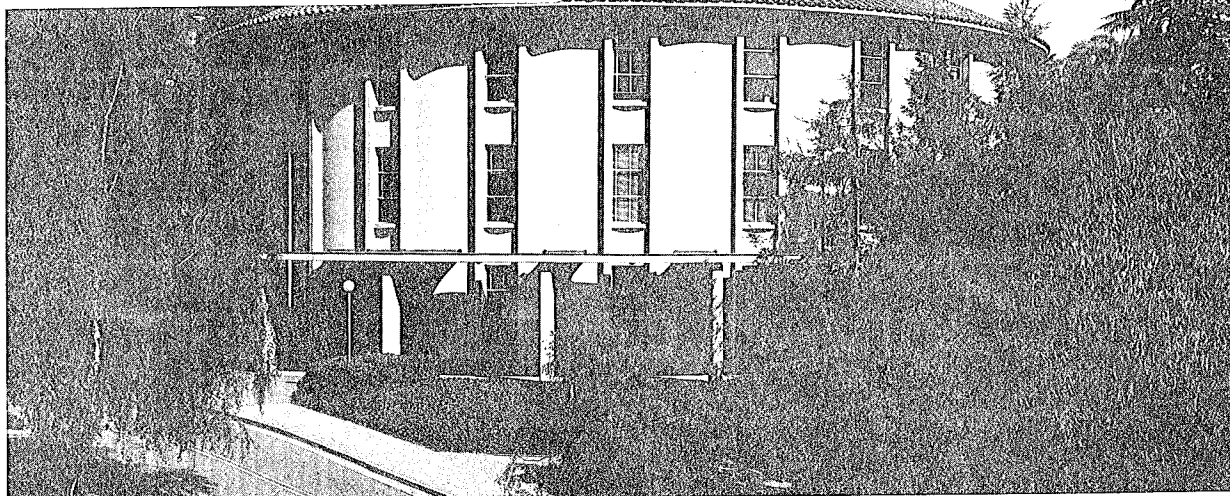
PHOTOVOLTAIC PROPERTIES OF AU-MEROCYANINE-TiO<sub>2</sub> SANDWICH CELLS  
II. PROPERTIES OF ILLUMINATED CELLS AND EFFECTS OF DOPING  
WITH ELECTRON ACCEPTORS

T. Skotheim, J.-M. Yang, J. Otvos, and M.P. Klein

July 1980

### TWO-WEEK LOAN COPY

*This is a Library Circulating Copy  
which may be borrowed for two weeks.  
For a personal retention copy, call  
Tech. Info. Division, Ext. 6782*



LBL-11231  
*c. 2*

Photovoltaic Properties of Au-Merocyanine-TiO<sub>2</sub>  
Sandwich Cells

II. Properties of Illuminated Cells and Effects of Doping  
With Electron Acceptors

T. Skotheim, J.-M. Yang, J. Otvos, and M.P. Klein

Laboratory of Chemical Biodynamics  
Lawrence Berkeley Laboratory  
University of California  
Berkeley, California 94720



## Abstract

Photocurrent generation in thin films of a merocyanine photosensitizing dye sandwiched between a  $\text{TiO}_2$  single crystal doped n-type and a Au overlayer has been studied using photovoltaic techniques. A theoretical model was developed to explain the observed photovoltaic properties. The model assumes that the principal route for the formation of charge carriers is via singlet excitons diffusing to the merocyanine- $\text{TiO}_2$  interface followed by dissociation of the excitons into electron-hole pairs, the electrons being injected into the  $\text{TiO}_2$  conduction band and the holes into the merocyanine. The model also incorporates field dependence of the quantum efficiency for charge generation. An exciton diffusion length of  $79 \text{ \AA}$  was determined by analyzing the short circuit action spectra using the theoretical model developed. The low fill factor of 0.35 for these cells was attributed to the field dependence of the quantum efficiency and the high series resistance of the undoped merocyanine films. Doping the merocyanine films with iodine was found to increase both the dark conductivity and the steady state photoconductivity, the latter by as much as a factor of five. This resulted in a quantum yield of 12% for a  $500 \text{ \AA}$  thick film and an increase in the fill factor to 0.44 giving a monochromatic power conversion efficiency of 0.4% at 520 nm.

The carrier generation in iodine doped films is shown to result from a bulk process, possibly involving collisions between singlet excitons and acceptor-hole complexes resulting in activation out of the bound states formed by the charge-transfer complex.

The quenching of excitons in the immediate vicinity of the metal surface was studied by monitoring the photoconductive response of a 200 $\text{\AA}$  merocyanine film with varying thickness of perylene sandwiched between the metal and the merocyanine. Perylene was shown to be able to transport the photoexcited holes from the merocyanine to the Au electrode. The quantum efficiency for photo-carrier production increased to a maximum of 21% for a 750 $\text{\AA}$  thick perylene layer.

## I. Introduction

This paper continues the discussion of the factors controlling the photovoltaic efficiencies of a sandwich cell made by interposing a thin film of a merocyanine photosensitizing dye between a  $\text{TiO}_2$  single crystal and a semitransparent Au overlayer (see article #1).

The previous paper reviewed the relevant literature and dealt with the electrical properties in the dark and the kinetic effects associated with the photoconductive response. The results were consistent with a junction model with an absence of free carriers and where the merocyanine acts as a dielectric between two electrodes. The photoconductive response was found to be determined by trapping effects.

The present report is concerned with the photovoltaic effects of merocyanine thin films sandwiched between  $\text{TiO}_2$  and Au electrodes. The power conversion efficiency of these devices is strongly dependent on the thickness of the merocyanine film. We shall show that the efficiency can be increased by doping the films with electron acceptors yielding monochromatic power conversion efficiencies of 0.4%. We have also investigated the quenching of the dye excitation by the Au electrode by interposing thin layers of perylene between the Au and the merocyanine. By using perylene as a spacer, we were able to obtain quantum yields as high as 21% by preventing the quenching of the excited merocyanine molecules by the metal surface.

We also present a theoretical model of the photoconductive charge transport in the merocyanine where the charge separation is assumed to take place exclusively at the merocyanine/ $\text{TiO}_2$  interface.

## II. Experimental

The thickness of the merocyanine film was varied from 200 to 3000 Å and the thickness of the gold film was 200 Å. The details of the fabrication are described in the previous article.

Only monochromatic light was used for the photovoltaic measurements. The light intensity was varied by using neutral density filters in front of the light source which was a 450 W Xenon lamp in conjunction with a Bausch and Lomb high intensity monochromator. The band width was 6 nm. The light intensity was always corrected for the O. D. of the TiO<sub>2</sub> or the Au film and represents light actually incident on the merocyanine film. The absorption spectra were recorded on a Cary 118 spectrophotometer.

## III. Results and Discussion

### A. Photo J-V Characteristics

1. Light Intensity Dependence of  $V_{oc}$  and  $J_{sc}$ . The photocurrent transients were described in the preceding article. Figure 1 shows the dependence on incident light intensity of the short circuit photocurrent ( $J_{sc}$ ) and the open circuit photovoltage ( $V_{oc}$ ) for a cell with a 500 Angstrom thick merocyanine film. It shows that the photocurrent varies linearly with the light intensity at least up to intensities of about  $10^{14}$  photons-sec<sup>-1</sup>-cm<sup>-2</sup> or about 0.1 mW-cm<sup>-2</sup>. For thicker cells, the light dependence of the photocurrent assumes the form  $J_{sc} \propto L^m$ ,  $L$  being the light intensity. The light exponent drops from unity to 0.93 for 2000 Angstrom-thick films. This relationship can be explained using a simple physical picture involving traps and recombination centers (1). As the light intensity is increased, the quasi-fermi level sweeps through trapping states located between the fermi level and the valence band and

converts them to recombination centers. As the light intensity is increased, more and more of the trapping states are converted to recombination centers. As the density of the recombination states increases, the life-time of the charge carriers decreases. This would result in a sublinear dependence of the photocurrent of the light intensity. For very thin films, the field across the dye layer is larger and charge separation consequently more efficient, less influenced by traps and recombination centers.

Figure 2 shows that the open circuit voltage ( $V_{oc}$ ) increases logarithmically with the intensity, and therefore also with  $J_{sc}$ . The behavior follows that expected for an abrupt junction (2),

$$V_{oc} = (mkT/q) \ln(J_{sc}/J_0 + 1)$$

where  $m$  is an empirical coefficient which is equal to 1 for an ideal junction and greater than 1 for non-ideal junctions with interface states, and  $J_0$  is the reverse saturation current. For a 500 Angstrom merocyanine cell,  $m = 1.71$ .

2. Photovoltage-Photocurrent Characteristics. The sign of the photovoltage of the Au-merocyanine- $TiO_2$  cells is such that the  $TiO_2$  is always negative. Fig. 3 shows the current-voltage characteristics of a cell with a 500 Angstrom thick dye film in the photovoltaic mode. The curve is obtained by varying the load resistance at a constant light intensity. The wavelength of the irradiation is 520 nm. The maximum power that can be extracted from a photovoltaic device is at the point for which the largest rectangle can be inscribed into the current voltage curve. The

maximum power output from this particular cell occurs with a load resistance of about  $5 \times 10^6$  ohms and is about  $5 \times 10^{-9}$  W. The incident light power on the active cell area is about  $5 \times 10^{-6}$  W, corrected for the O. D. of the  $\text{TiO}_2$  crystal. The power conversion efficiency at this light level is therefore about 0.1%.

The fill factor is defined as the ratio of maximum output power to the product of  $V_{oc}$  and  $J_{sc}$  and gives a measure of how close the cell is to an ideal solar cell. The fill factor for this cell is 0.35 compared to 0.75 - 0.8 for Si and GaAs solar cells (3). The low fill factor is probably due to two separate effects. High series resistance will lower the fill factor by lowering the output voltage for a given output current (4). In addition, the field dependence of the photocurrent would lead to a lowering of the output current for a given output voltage, since the photovoltage would work against the built-in charge separating field. At low quantum yields, the second effect is probably dominant (5).

3. Open Circuit Voltage. The total potential drop across the junction region is determined by the difference between the work functions of the Au and the semiconductor. If the work function of Au is taken as 4.85 eV (6) and the work function of  $\text{TiO}_2$  as 4.33 eV (7), we get a built-in voltage,  $V_D$ , of 0.52 eV. We take the work function of the  $\text{TiO}_2$  to be the same as the electron affinity of the crystal, since the donor density is high ( $10^{18} \text{cm}^{-3}$ ), and the fermi level consequently lies close to the conduction band. In principle,  $V_{oc}$  should approach  $V_D$  under conditions of intense illumination. The highest open circuit voltage measured under monochromatic irradiation was 375 mV. The incident light intensity was about  $0.1 \text{ mW-cm}^{-2}$ .

## B. Photovoltaic Action Spectrum

Figure 4 shows the absorption spectrum of a 1000 Angstrom merocyanine dye film on quartz and the photovoltaic action spectrum of a Au-merocyanine-TiO<sub>2</sub> cell with a 1000 Angstrom film. For the action spectrum, the light was incident on the TiO<sub>2</sub> crystal. The value of the photocurrent has been normalized by the relative photon flux at each wavelength and corrected for the O. D. of the crystal. It can be seen that the photocurrent action spectrum essentially matches the absorption spectrum of the film.

Figure 5 shows the absorption and photocurrent action spectra for a cell with a 2000 Angstrom film of merocyanine with light incident on the Au overlayer. The spectrum has been corrected for incident photon flux. Illumination through the gold generates peaks in the action spectrum at wavelengths on the shoulders of the absorption spectrum. In addition, the quantum yield is more than two orders of magnitude less than with illumination through the TiO<sub>2</sub>. The polarity of the cell is the same regardless of which side is being illuminated. Such photocurrent action spectra where the action spectrum agrees with the absorption spectrum for light incident only through one electrode and with a local minimum near the peak of absorption for light incident through the opposite electrode, have been observed for a number of organic systems (5,8,9,10,11). This effect is not seen for very thin films where the absorption is essentially uniform throughout the dye layer. Fig. 6 shows the absorption spectrum and the action spectrum with light incident on the Au as well as the action spectrum with light incident on the TiO<sub>2</sub> for a cell with a 100 Angstrom thick merocyanine film. As can be seen, they both essentially match the absorption spectrum of the merocyanine film. The absorbance was about 0.1 at the peak of the spectrum.

These results are in accord with a theory of the photoconductivity process, which will be elaborated below, where the photovoltaic activity is

a surface effect. The photoconductivity is assumed to result from singlet excitons diffusing to the merocyanine/TiO<sub>2</sub> interface where they dissociate into electron-hole pairs which separate in the electric field across the dye layer in competition with geminate recombination. Only those excitons which migrate to the merocyanine/TiO<sub>2</sub> interface contribute to the photocurrent.

For light incident on the Au electrode, the higher the absorption constant the closer to the metal surface the excitons will be generated on the average where the quenching of the excitation is very efficient. For light with lower absorption constant, away from the peak of absorption, the excitons will be on the average generated closer to the merocyanine/TiO<sub>2</sub> interface where the charge separation takes place, and consequently a larger photocurrent results. A weak photovoltaic response is also seen for wavelengths of weak absorption, because the penetrating light is not effective.

### C. Photoconductivity of Merocyanines

1. Theory of Exciton Transport. In most inorganic semi-conductors, the generation of photocarriers is a simple process whereby the absorbed photon with energy greater than the band gap excites an electron-hole pair directly. In molecular solids, the generation is more complex. In general, the photoconduction action spectrum is identical to the absorption spectrum. The absorption spectra of organic molecular solids can be understood in terms of Frenkel excitons which are described in the tight binding approximation (12).

The size of the Frenkel exciton is comparable to lattice constants and it is expected to have low mobility. This is what one typically finds in molecular solids where the mobility is usually less than  $1 \text{ cm}^2\text{-V}^{-1}\text{-sec}^{-1}$ . Because they are localized, they also interact with molecular vibrations as well as lattice vibrations. The original exciton can produce charge carriers

via several mechanisms (13). The possible mechanisms include exciton-exciton interactions, interaction of excitons with free and trapped charges and defect states, and exciton-surface processes. We have found that the merocyanine photoconductivity data can best be explained by the theory of exciton-surface processes whereby only excitons reaching the merocyanine-TiO<sub>2</sub> interface contribute to the photocurrent. In this section we briefly review the theory of exciton surface processes. Experimental results supporting this theory will be presented below.

Excitons can diffuse to the surface and dissociate upon collision with adsorbed oxygen, impurities, defects, and/or electrodes. The photocurrent resulting from the exciton dissociation will be linear in light intensity, since the process is monomolecular in nature. An analysis of exciton diffusion and surface interaction was carried out by Stekette and de Jonge (14) and by Mulder (15) for anthracene crystals and by Ghosh and Feng (5) for merocyanine.

One can obtain a quantitative relationship between the steady state photocurrent and the absorption coefficient by calculating the probability of an exciton reaching the surface by diffusion. It is assumed that the exciton has a certain mean lifetime (due to fluorescence and non-radiative transitions) and that its motion can be described as a free diffusion process. The exciton transport can then be described by the diffusion equation which in this system is essentially one-dimensional

$$0 = \frac{\partial n(x)}{\partial t} = D \frac{\partial^2 n(x)}{\partial x^2} - \frac{n(x)}{\tau} + \alpha I_0 e^{-\alpha x} \quad 3.7.1$$

for the stationary state.  $n$  is the number of excitons at a distance  $x$  from the illuminated surface,  $D$  is the diffusivity,  $\tau$  is the mean lifetime of an

exciton,  $\alpha$  is the absorption constant, and  $I_0$  the photon intensity of the incident light. The second term on the right represents recombination due to all processes and the third term generation of excitons. If we assume that all the excitons reaching the surface dissociate there, the boundary conditions become  $n(0) = 0$  and  $n(d) = 0$  where  $d$  is the thickness of the film. Solving equation (3.7.1) with these boundary conditions, we obtain (14)

$$n(x) = \frac{I_0 \alpha \tau}{1 - \alpha^2 D \tau} \left\{ \exp(-\alpha x) + \frac{\exp\left(\frac{x}{L}\right) \left[ \exp\left(-\frac{d}{L}\right) - \exp(-\alpha d) \right] - \exp\left(-\frac{x}{L}\right) \left[ \exp\left(\frac{d}{L}\right) - \exp(-\alpha d) \right]}{\exp\left(\frac{d}{L}\right) - \exp\left(-\frac{d}{L}\right)} \right\} \quad 3.7.2$$

where  $L = \sqrt{D\tau}$  is the diffusion length of the exciton.

The details of the interaction between the excitons and the surface electrode determines whether the exciton dissociation at the surface will lead to charge separation and a photocurrent. At the charge separating electrode, we assume that the photocurrent is directly proportional to the exciton flux at the surface, i.e. the quantum efficiency for charge generation is assumed constant,

$$J = A \frac{\partial n(0)}{\partial x} \quad 3.7.3$$

where the proportionality constant  $A$  depends on the nature of the electrode.

If we make the further assumption that  $d > L$ , then  $\exp(d/L) \gg \exp(-d/L)$ , and we obtain for the photocurrent

$$J = \frac{A}{D} \frac{I_0}{1/\alpha L + 1} \quad 3.7.4$$

or

$$1/J = 1/J_\infty (1 + 1/\alpha L) = 1/J_\infty (1 + 0.434/\epsilon L) \quad 3.7.5$$

where  $\epsilon$  is the extinction coefficient defined by  $I_x = I_0 10^{-\epsilon x}$ . From equation (3.7.5) we see that a plot of  $1/J$  versus  $1/\alpha$  should give a straight line.

2. Experimental Results. In Fig. 7 the reciprocal photocurrent, which has been normalized by the relative photon flux at each wavelength, is plotted versus the reciprocal absorption constant for wavelengths greater than 420 nm. The thickness of the merocyanine film was 2000 Angstroms. As can be seen, using a least squares approximation, a well-fitting straight line can be drawn. Using equation (3.7.5), the slope of the line and the intercept on the ordinate yield an exciton diffusion length of 79 Angstroms. This is in fair agreement with Ghosh and Feng (5), who calculated a diffusion length of 60 Angstroms.

#### D. Field Dependence of the Quantum Efficiency

Fig. 8 shows the dependence of the photocurrent on an applied electric field. The cell is reverse biased, i.e. a positive potential is applied to the  $TiO_2$ . The dark current has been subtracted from the total current. The curve exhibits a knee followed by a sharp increase at about 0.75 volts for this particular sample with a 500 Angstrom thick dye film. The voltage of the transition increases for increasing film thickness. The photocurrent at

the knee corresponds to a quantum yield of about 15% where the quantum yield is defined as the number of charges generated per photon absorbed by the merocyanine film. With 1 volt or more applied bias, the quantum yield increases to more than 100%. The sudden increase in photocurrent must therefore be due to secondary charges injected by the electrodes. For thicker films a larger applied voltage would be required to produce the same internal electric field.

Our data supports the theory that only excitons that reach the merocyanine/TiO<sub>2</sub> interface produce free charge carriers. The absence of charge generation at the merocyanine/Au interface can be the result of a combination of two different processes. Excited dye molecules in the immediate vicinity of a metal surface can be quenched very effectively via radiative and non-radiative interaction with the metal (16-19). Secondly, the excitons which do dissociate will be lost to geminate recombination, since the dissociation would not be at the surface itself but removed a certain distance corresponding to the effectiveness of the quenching (19).

Fig. 9 shows the quantum yield as a function of the thickness of the merocyanine film. The measurements are recorded at the peak of the photocurrent action spectrum with light incident on the TiO<sub>2</sub>. The decrease in quantum yield for thicker films is mainly due to the decrease of the electric field across the merocyanine as the film thickness increases. The decrease in efficiency when the film is less than about 350 Angstroms we believe is due to the quenching of the dye excitation via interaction with the metal surface. This quenching effect takes place over distances typically of the order of 200-300 Angstroms and is influenced by the introduction of a second partially reflecting mirror, in this case the merocyanine/TiO<sub>2</sub> interface (19). The quenching effect will be discussed in

more detail below.

The field dependence of the photocurrent can be understood by application of a one-dimensional solution to the Onsager theory for geminate recombination as applied by Singh and Baessler to the Al-anthracene interface (20). The Onsager theory considers the brownian motion of a charged particle under the combined action of an external electric field and the coulombic field of its counter charge (21). In the Au-merocyanine-TiO<sub>2</sub> cells, the dissociation of excitons at the merocyanine/TiO<sub>2</sub> interface results in the injection of a free hole into the merocyanine with a negative image charge in the TiO<sub>2</sub> conduction band. In the course of correlated brownian motion, both charges can either recombine or become separated. The orientation of the charge-image charge dipole is in this case always parallel to the direction of the applied field which is the built-in field due to the original difference in fermi levels in addition to any applied bias.

These results also suggest that one way to increase the efficiency of cells of this type would be to choose metal-semi-conductor combinations with larger differences between the electrochemical potentials than is the case for Au and TiO<sub>2</sub>.

#### E. Doping of Merocyanine Films with Iodine

1. Introduction. There have been numerous reports in the literature of sharp increases of photoconductivity as well as dark conductivity in organic solids doped with electron acceptors (22-25). Intentionally doping semiconductor materials with trace impurities in order to alter photoelectronic properties is used extensively and is well understood in inorganic solar cell technology. In organic solids the complex relationships between dopant

types and concentrations and photoelectronic properties are just beginning to be studied. Dramatic changes in the photoconductive properties of p-type organic solids have been reported. As much as four orders of magnitude increases in the photoconductivity of phthalocyanine surface cells with a layer of iodine added has been reported (23).

The original work on doping with electron acceptors used a surface cell technique whereby the conductivity of a two-layer system with a layer of the acceptor species deposited on top of the material to be investigated, was measured along the film (22- 25). There was no attempt made to determine whether the acceptor species diffused into the substrate or whether the effect was purely a surface effect.

2. Experimental. Because of the high vapor pressure of iodine, its use in high vacuum necessitates the deposition on cooled substrates. Iodine films deposited onto room temperature substrates come off under high vacuum in a matter of a few minutes. Since iodine doping of dye films is a reversible reaction--the iodine can be completely removed by pumping in vacuum--it becomes necessary to cool the dye film to prevent the iodine from escaping while the cell is being prepared.

The best results to date have been achieved with the following technique: Prior to the sublimation of the iodine, the  $TiO_2$  crystal is exposed to iodine vapor at room temperature and atmospheric pressure for about fifteen minutes. This leaves a visibly brown film on the surface. The crystal is then quickly cooled to liquid nitrogen temperature with the substrate cooling system as the vacuum is being pumped down to prevent moisture in the air from condensing on the surface. The brown iodine film will remain on the surface in a vacuum of  $10^{-5}$  torr for as long as is necessary to prepare the cell. The merocyanine is then sublimed on top of the

iodine film at a rate of about 2 Angstroms per second from a crucible held at approximately 220°C. The substrate could then be heated to room temperature followed by deposition of the Au film or heated after the Au film was deposited. Standard photovoltaic measurements were then made on the cell. The cell was subsequently placed in vacuum and heated to 60°C for thirty minutes followed by photovoltaic measurements. This was repeated several times until a maximum value was reached for the photovoltaic response. The idea was to use the increased diffusivity of iodine at elevated temperatures to attempt to diffuse the I<sub>2</sub> throughout the dye film.

3. Results and Discussion: Transient Response. Fig. 10 shows the short circuit and open circuit voltage transients for a typical iodine doped cell. The J<sub>sc</sub> transient is dramatically different from that of the undoped cells (see Part I). The rise time as well as the decay time are now limited solely by the response of the recorder, whereas the risetime of undoped cells is typically of the order of tens of seconds reaching a steady state. This is sometimes followed by a slow decay to a level about 20% lower than the peak with a time constant of the order of an hour. The slow decay for doped cells is always present and has a time constant of the order of minutes, also resulting in a level approximately 20% lower than the peak transient. The exact numbers vary slightly from cell to cell depending upon the history. On switching off the light, the decay results in a small reverse current indicating the presence of capacitive charging effects.

The open circuit voltage also exhibits a faster rise and decay time for the doped cells, the change being less dramatic because the response in this case is limited by the large time constant of the measuring circuit, the resistance in the open circuit mode being about 10<sup>14</sup> ohms.

Action Spectra. The action spectrum of the short circuit photocurrent is shown in Fig. 11 for a cell with a 500 Angstrom thick merocyanine film doped with iodine with the technique described above. The cell had been heat treated in vacuum for 1 1/2 hours. With further heat treatment in vacuum, the cell reverts to undoped behavior. This indicates that the vacuum treatment indeed does make the iodine diffuse through the merocyanine film and also through the 200 Angstrom thick Au film.

As can be seen, the shape of the action spectrum changes only slightly upon doping. The quantum efficiency increased by approximately a factor of 3, from 4% to about 12%. Increases by as much as a factor of 5 have been noticed on some films. The open circuit voltage increased usually by much less; the best result represents an increase by a factor of 1.8 with a 500 Angstrom merocyanine film. The effect of the doping was more pronounced for thinner films (500 Angstroms and less) than for thicker films (1000 Angstroms and greater). The results, however, were difficult to reproduce to better than within a factor of 2.

When the reciprocal short circuit photocurrent normalized to incident photon flux is plotted versus the reciprocal absorption constant, the results do not give a good fit to a straight line as in the case with undoped merocyanine films. An attempt to obtain a least squares fit yields an exciton diffusion length of 2300 Å. This is an unreasonable number, since the diffusion length in very pure organic crystals is usually less than 1000 Å (28). This indicates that a different charge carrier mechanism may be operative. The increased dark conductivity of doped films would be expected to result in a larger degree of band bending in the semiconductor substrate and therefore more efficient charge generation by intrinsic absorption of photons with energy larger than the band gap. This has indeed been noticed

and increases by about a factor of three were noticed on some cells.

The improved efficiency, however, degraded slowly with time. The doped films, on standing overnight under ambient atmospheric conditions, reverted to their undoped behavior.

The vacuum heat treatment shows that there is an optimum dopant concentration. When the cells are too heavily doped, the photovoltaic properties were completely degraded. The exact amount of doping or the doping profile in the merocyanine films was not measurable.

Photovoltage-Photocurrent Characteristics. Fig. 12 shows the J-V characteristics in the photovoltaic mode of a Au-merocyanine-TiO<sub>2</sub> cell with a 500 Angstrom I<sub>2</sub> doped film. The J-V curve for an undoped film is also shown for comparison. The curve is obtained by varying the load resistance at a constant light intensity at 520 nm.

Besides the increases in  $J_{sc}$  and  $V_{oc}$ , the curvature of the cell also changes. This leads to an increase in the fill factor from 0.35 for an undoped cell to 0.44 for the I<sub>2</sub> doped cell. The maximum power output from this cell occurs with a load resistance of about  $5 \times 10^6$  ohms and is about  $2 \times 10^{-8}$  W. The incident light power on the active cell area was about  $5 \times 10^{-6}$  W. This yields a monochromatic power conversion efficiency of about 0.4% which is an increase by a factor of four relative to undoped cells.

#### F. Quenching of Dye Excitation at the Metal Surface

1. Introduction. We showed above that the quantum efficiency for photocarrier generation drops for merocyanine thicknesses of less than about 350 Å. This was attributed to the quenching of the dye excitation by the interaction with the metal surface.

The influence of a metallic mirror on an excited molecule in its

immediate vicinity has been extensively studied during the past few years (16-19, 26). Using fatty-acid monolayer assembly techniques, the fluorescence lifetime of Europium complexes has been measured as a function of its distance from metal surfaces. One finds that for larger distances ( $> 2000 \text{ \AA}$ ) the fluorescence lifetime oscillates around its free molecule value while for small distances ( $< 200 - 300 \text{ \AA}$ ) the lifetime goes monotonically to zero.

We decided to investigate this quenching effect on the merocyanine film by introducing a spacer of various thicknesses between the merocyanine and the Au electrode. The spacer would have to be a hole conductor for the photo-generated hole carriers in the merocyanine film. Perylene was chosen because it is known to be a p-type conductor with an ionization energy of 5.33 eV (27), which is sufficiently less than the ionization energy of the merocyanine which is in the range 5.6 - 5.8 eV (28). A model of the energy level diagram can then be schematically represented as in Fig. 13.

2. Experimental. Perylene was purchased from Aldrich Chemical Company and used without further purification. The cells were made by sequential sublimation from molybdenum boats in a vacuum of  $10^{-5}$  torr. The temperature of the perylene powder was held at about  $180^\circ\text{C}$ . The deposition rate was about  $2 \text{ \AA-sec}^{-1}$ . The details of the fabrication procedure have been described previously (see Part I).

3. Results. The perylene films were smooth and glassy in appearance and were transparent in the visible when deposited onto room temperature substrates. The characteristic absorption bands of the free molecule in solution disappears in the film. This was also observed by Kamura, et al. (29) and attributed to a dichroism effect on microcrystals with a preferred orientation.

Fig. 14 shows the effect of the perylene layer on the photocurrent response for a cell with a 200 Angstrom merocyanine film. The quantum yield, measured as the number of electrons per photon absorbed by the merocyanine, is plotted as a function of the thickness of the perylene layer for one particular  $\text{TiO}_2$  crystal. As can be seen, the quantum yield increases approximately five-fold to about 21% for a perylene layer of 750 Angstroms.

The slight decrease in efficiency for a thickness of 1500 Å could be attributed to decreasing field strength across the dye layer with a possible contribution from the oscillatory nature of the excitation lifetimes at larger distances. The increase in quantum yield is even more striking in light of the fact that the electric field at the junction decreases with increasing perylene thickness.

In order to determine the charge separating properties of the perylene-merocyanine interface, we compared the action spectrum of a cell having a 1000 Angstrom perylene film between a 2000 Angstrom merocyanine film and the Au electrode with a similar cell without the perylene but with the same thickness of the merocyanine. With an absorbance of 2.0 and an exciton diffusion length of less than 100 Angstroms, the charge carrier generation will be that due to exciton dissociation at the perylene-merocyanine interface. Fig. 15 shows the action spectra for the two cells recorded with light incident on the Au surface. Although the action spectra are similar in shape, the local minimum near the peak of the absorption as well as the peaks on the shoulders are less pronounced in the cell with perylene. The local minimum was attributed to a quenching of the excitation near the Au-merocyanine interface. The quenching effect remaining at the perylene-merocyanine interface is probably due to the lack of an electric field at the interface strong enough to substantially overcome the coulombic

forces resulting in geminate recombination. This effect appears to be independent of the ability of the interface to transmit photoproduced holes from the merocyanine phase.

This could have important implications for the concept of extending the absorption range of organic systems by employing multilayers of dye films. Unless by doping and other methods one is able to initiate charge separation in the bulk of the dye phase, the interfaces between the layers may well be too inefficient to serve that purpose. Dye mixing as well as doping may turn out to be the more fruitful approach.

#### IV. Discussion

The experimental results presented in the preceding sections suggest that there are ways to utilize in photoelectric devices very thin films of organic pigments having a high electron transfer efficiency.

From the correspondence between the absorption spectra and the spectral response of photoconduction, it is concluded that the primary step is the formation of singlet excitons by the absorption of light. This excitation energy may migrate through the film as an exciton, traveling an average distance of about 80 Angstroms before it dissociates or is quenched. Only excitons reaching the merocyanine-TiO<sub>2</sub> interface actually result in charge carriers. The dissociation of the exciton leads to an electron being injected into the conduction band of the TiO<sub>2</sub> and a hole injected into the merocyanine. The hole then travels through the merocyanine to the Au electrode.

The charge carrier generation is presumed to result from a competition between the electric field at the interface and the coulombic attraction between the electron and the hole. The mechanism, we believe, is therefore

the one described by Onsager's theory of geminate recombination adapted to the present one-dimensional system.

The Au-merocyanine interface is ineffective for charge carrier generation due to a quenching of the excitons in the immediate vicinity of the metal surface and possibly a reduced internal electric field near the interface.

If the semiconductor substrate is to be used as a separate absorber generating mobile charges by intrinsic excitation, the dark conductivity of the dye phase must be increased to semiconductor conductivities in order to generate a depletion region in the semiconductor. This can be achieved by introducing the concepts of doping and charge transfer complexes. Our experiments with doping of the merocyanine with iodine shows that in addition to this effect, the photoconductivity of the merocyanine was increased as well. The accompanying increase in photovoltage is probably a result of larger photocurrent. Increases in photocurrent generation by as much as five-fold relative to the undoped cells were recorded.

The doping with iodine had the potential for both enhancing the conductivity of the films by introducing partial charge transfer or mixed valence states and for providing favorable surface state band bending which could lead to higher output voltage. The concept of partial charge transfer has been used to explain doping effects in molecular conductors (24,25, 30-32) and in conductive polymers (33,34). Raman studies of iodine doped polyacetylene (33) and phthalocyanines (25) have identified the presence of  $I_3^-$  as the dominant species resulting in charge transfer from the organic state to the iodine as an acceptor. The charge transfer need not be complete. The resulting hole is weakly bound to the acceptor ions by the coulombic potential, forming acceptor states in the gap. Thermal activation

out of the bound states results in carriers for transport. Photocarriers in doped films could result from collision of singlet excitons with acceptor-hole complexes resulting in activation out of the bound states and recombination of the exciton. The charge carrier generation therefore changes to a bulk process.

The greatly decreased rise and decay time constants of the photocurrent and photovoltage response indicate that the presence of iodine fundamentally changes the nature and concentration of trapping states in the merocyanine. The continued presence of the slow decay with a decreased time constant of the photocurrent to a level about 20% lower than the peak value indicates that it may be a surface controlled capacitive charging effect. The absence of a reverse current upon turning off the light in the case of the undoped films (see Part I) can be explained by the large time constant of the decay dominating the reverse capacitive discharge, the two being separate processes.

Despite the preliminary nature of these experiments, it is clear that increases in efficiency of at least five-fold can readily be obtained. It is hoped that a better understanding of donor-acceptor complexes and other dopants could result in even higher potential efficiency increases.

Very thin films would be expected to be the most efficient for charge injection both because of the limitations on the exciton diffusion length in the case of the undoped films, and the increase in the electric field strength due to the built-in voltage. For films of a few hundred Angstroms, however, the excitation is partially quenched by the interaction with the metal surface. The interaction takes the form of non-radiative energy transfer to the metal for short distances. The states which accept the energy are the surface plasmons of the metal-dielectric interface (19,35).

This quenching effect was investigated by sandwiching perylene layers of varying thickness between the merocyanine and the Au for cells with a 200 Å merocyanine film. We found a dramatic improvement in the photoconductive response as the merocyanine was displaced from the metal surface resulting in increases of as much as five-fold for a perylene thickness of 750 Å. This increase is even more remarkable as the electric field strength across the dye layer decreases sharply as the thickness of the perylene is increased.

The long-term stability under ambient atmospheric conditions is an important problem which has to be addressed with constructing devices based on organic solids. Our research has not been concerned with long-term stability beyond two to three days, although the merocyanine films did degrade over such a period. Careful encapsulation as well as employment of polymerized compounds may be able to produce devices with the necessary longevity.

Our research to date shows that there are ways to utilize the optoelectronic properties of very thin organic films with a high probability for charge generation. It seems likely, therefore, that the low yields achieved to date for organic photovoltaic systems may be more due to device limitations than limitations intrinsic to organic materials as a class.

#### Acknowledgements

We are grateful to the Division of Chemical Sciences, Office of Basic Energy Sciences of the United States Department of Energy for support of this work under Contract W-7405-ENG-48. This paper was printed by original provided by the author.

## References

1. A. Rose, "Concepts in Photoconductivity and Allied Problems," (New York: Interscience, 1963).
2. S. M. Sze, "Physics of Semiconductor Devices," (New York: Wiley, 1969).
3. H. J. Hovel, "Solar Cells," Vol. 11 in the series "Semiconductors and Semimetals," R. K. Willardson and A. C. Beer, eds. (New York: Academic Press, 1975).
4. J. J. Wysocki, RCA Review 22, 57 (1961).
5. A. K. Ghosh and T. Feng, J. Appl. Phys. 49, 5982 (1978).
6. CRC Handbook of Chemistry and Physics, 52nd ed. (1971).
7. M. A. Butler and D. S. Ginley, J. Electrochem. Soc. 125, 228 (1978).
8. A. K. Ghosh and T. Feng, J. Appl. Phys. 44, 2781 (1973).
9. C. W. Tang and A. C. Albrecht, (a) Mol. Cryst. Liq. Cryst. 25, 53 (1974); (b) J. Chem. Phys. 62, 2139 (1975); (c) J. Chem. Phys. 63, 953 (1975); (d) Nature 254, 507 (1975).
10. A. K. Ghosh, D. L. Morel, T. Feng, R. S. Shaw, and C. A. Rowe, J. Appl. Phys. 45, 239 (1974).
11. F. R. Fan and L. R. Faulkner, (a) J. Chem. Phys. 69, 3334 (1978); (b) J. Chem. Phys. 69, 3341 (1978).
12. R. S. Knox, "Theory of Excitons, Solid State Physics Series," Supplement 5, F. Seitz and D. Turnbull, eds. (Academic Press: New York, 1963).
13. H. Inokuchi and Y. Maruyama, "Photoconductivity and Related Phenomena," J. Mort and D. M. Pai, eds. (Elsevier Scientific: New York, 1976).
14. J. W. Stekette and J. de Jonge, Philips Res. Rep. 17, 363 (1962).
15. B. J. Mulder, Philips Res. Rep. Supplement 4 (1968).

16. K. H. Drexhage, H. Kuhn, and F. P. Schafer, Ber. Bunsenges. Phys. Chem. 72, 329 (1968).
17. K. H. Drexhage, H. Fleck, H. Kuhn, F. P. Schafer, and W. Sperling, Ber. Bunsenges. Phys. Chem. 20, 1179 (1966).
18. K. H. Drexhage, J. Luminescence 1/2, 693 (1970).
19. R. R. Chance, A. Prock, and R. Silbey, (a) J. Chem. Phys. 62, 2245 (1975); (b) Ibid. 65, 2527 (1976); (c) Adv. Chem. Phys. 37, 1 (1978).
20. J. Singh and H. Baessler, Phys. Stat. Sol. (b) 63, 425 (1974).
21. L. Onsager, Phys. rev. 54, 554 (1938).
22. D. R. Kearns and M. Calvin, J. Chem. Phys. 29, 950 (1958).
23. D. R. Kearns, G. Tollin, and M. Calvin, J. Chem. Phys. 32, 1020 (1960).
24. H. Akamatu, H. Inokuchi, and Y. Matsunaga, (a) Nature 173, 108 (1954); (b) Bull. Chem. Soc. Japan 29, 213 (1956).
25. J. L. Peterson, C. S. Schramm, D. R. Stojakovic, B. M. Hoffmann, and T. J. Marks, J. Am. Chem. Soc. 99, 286 (1977).
26. H. Killesreiter, J. Luminescence 12/13, 857 (1976).
27. B. Korsch, F. Illig, H. J. Gaehrs, and B. Tesche, Phys. Stat. Sol. (a) 33, 461 (1976).
28. H. Meier, "Organic Semiconductors," (Weinheim: Verlag Chemie, 1974).
29. Y. Kamura, I. Shirovani, K. Ohno, K. Seki, H. Inokuchi, Bull. Chem. Soc. Japan 49, 418 (1976).
30. W. Mehl and N. E. Wolff, J. Phys. Chem. Solids 25, 1221 (1964).
31. L. B. Coleman, M. J. Cohen, D. J. Sandman, F. G. Yamagishi, A. F. Garito, and A. J. Heeger, Solid State Commun. 12, 1125 (1973).
32. E. M. Engler, R. A. Craven, Y. Tomkiewicz, and B. A. Scott, J. Chem. Soc. Chem. Commun., 337 (1976).

33. C. K. Chiang, Y. W. Park, A. J. Heeger, H. Shirakawa, E. J. Louis, and A. G. MacDiarmid, *J. Chem. Phys.* 69, 5098 (1978).
34. I. B. Goldberg, H. R. Crowe, P. R. Newman, A. J. Heeger, and A. G. MacDiarmid, *J. Chem. Phys.* 70, 1132 (1979).
35. H. Morawitz and M. R. Philpott, *Phys. Rev. B* 10, 4863 (1974).

## FIGURE CAPTIONS

- Figure 1. Light intensity dependence of short circuit current and open circuit voltage for a cell with 500 $\text{\AA}$  merocyanine.
- Figure 2. Semi-log plot of the light intensity dependence of the open circuit voltage.
- Figure 3. Photocurrent-photovoltage characteristics for a cell with 500 angstrom merocyanine film. Irradiation at 520 nm.
- Figure 4. Short-circuit photocurrent, normalized to incident photon flux, for light incident on the  $\text{TiO}_2$ , and absorption spectrum of the merocyanine. The thickness of the merocyanine film was 1000 angstroms.
- Figure 5. Short-circuit photocurrent and absorption spectrum with light incident through the Au electrode. The photocurrent was normalized to incident photon flux. The thickness of the merocyanine film was 2000 angstroms.
- Figure 6. -.-. Absorption of merocyanine film.  $\Delta$  - short circuit photocurrent with light incident through the Au electrode. 0 - Short-circuit photocurrent with light incident through the  $\text{TiO}_2$ . The thickness of the merocyanine film was 100 angstroms. The two photocurrent action spectra were normalized to incident photon flux.
- Figure 7.  $I/J$  versus  $1/\alpha$  plot of short-circuit photocurrent for wavelengths greater than 420nm. The photocurrent has been normalized by the relative photo flux at each wavelength. The thickness of the merocyanine film was 2000 angstroms.
- Figure 8. Photocurrent versus applied reverse bias for a cell with a 500 angstrom merocyanine film under 520nm monochromatic illumination. The polarity of the  $\text{TiO}_2$  was positive.
- Figure 9. The quantum yield, measured as the number of electrons per photon absorbed by the merocyanine, is plotted as a function of the thickness of the merocyanine. The quantum yield was measured with monochromatic illumination at 520nm in the short circuit mode.
- Figure 10. Short-circuit current and open circuit voltage transients for a cell with a 500 angstrom merocyanine film doped with iodine. The light was incident through the  $\text{TiO}_2$ .
- Figure 11. Short circuit photocurrent action spectrum for a cell with a 500 angstrom merocyanine film doped with iodine and a cell with a 500 angstrom undoped film. Also shown is the absorption spectrum of the undoped film.

- Figure 12. Photovoltage-photocurrent characteristics for a cell with a 500 angstrom merocyanine film doped with iodine and a cell with a 500 angstrom undoped film.
- Figure 13. Energy level representation of a Au-erylene-merocyanine-TiO<sub>2</sub> cell under short circuit condition.
- Figure 14. Quantum yield for a Au-erylene-merocyanine-TiO<sub>2</sub> cell plotted as a function of the thickness of the erylene layer. The thickness of the merocyanine was 200 angstroms.
- Figure 15. Short circuit photocurrent action spectrum with light incident through the Au electrode for a cell with a 1000 angstrom erylene layer and a cell with no erylene. The action spectra were normalized to incident photon flux at each wavelength. The thickness of the merocyanine was 2000 angstroms.

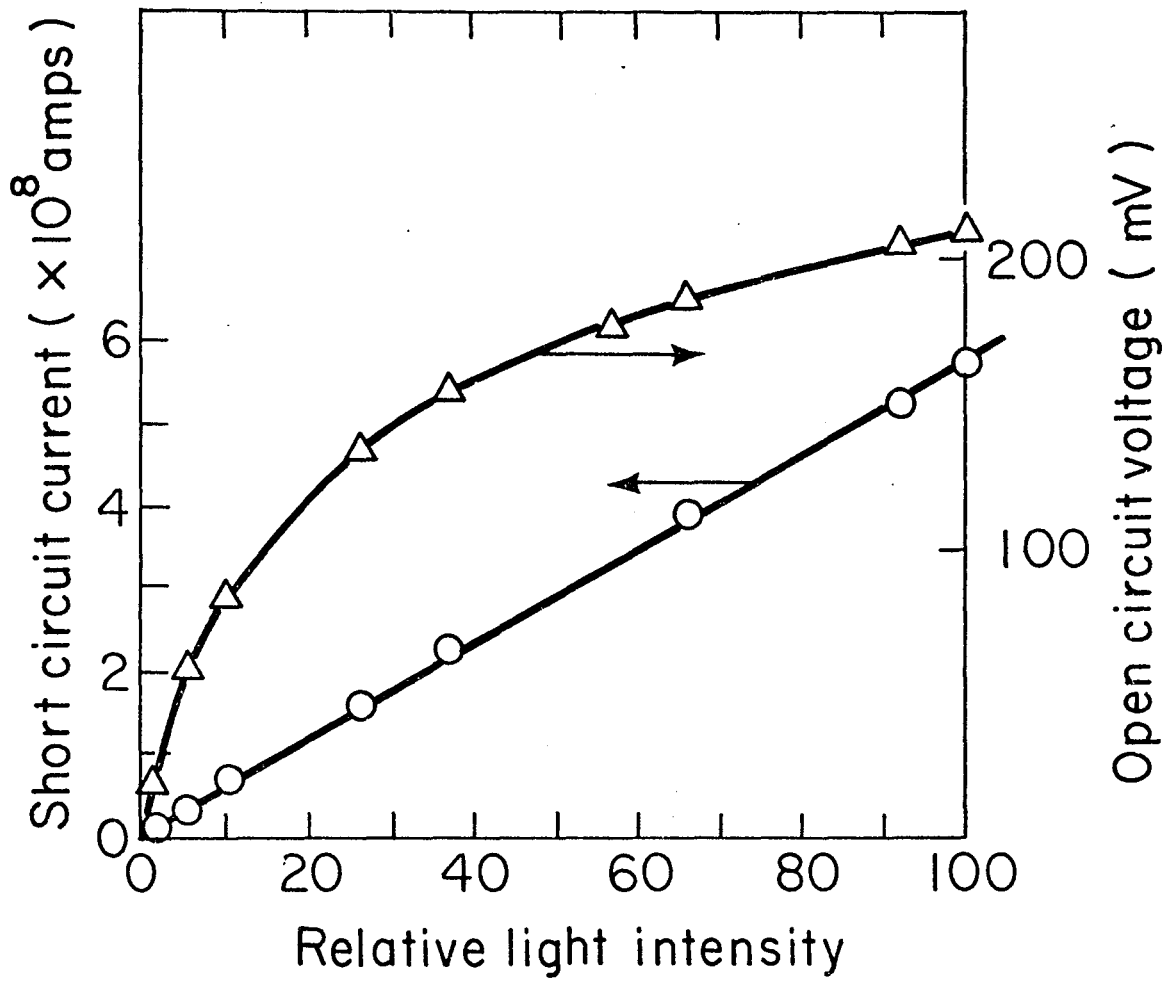


Fig. 1

XBL797-4887

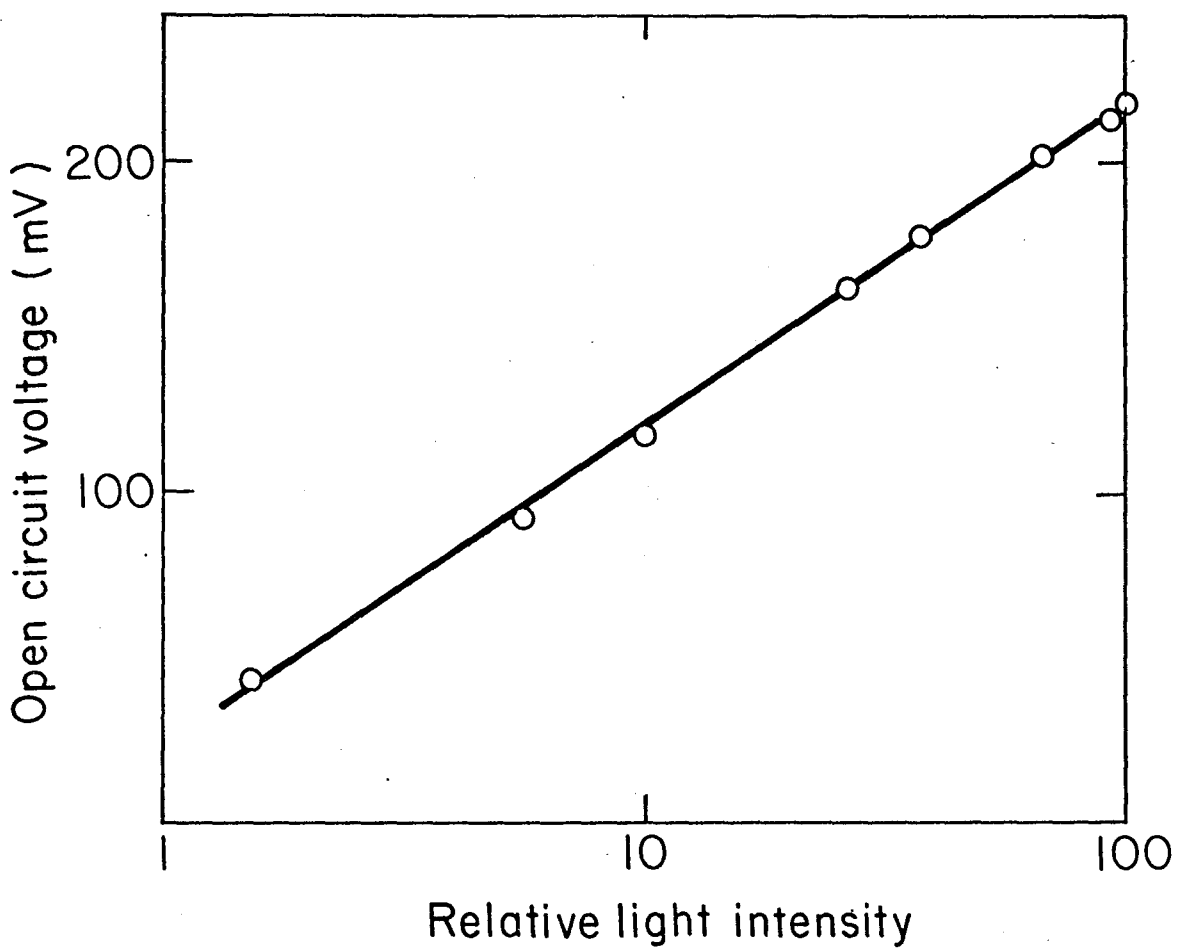


Fig. 2

XBL797-4891

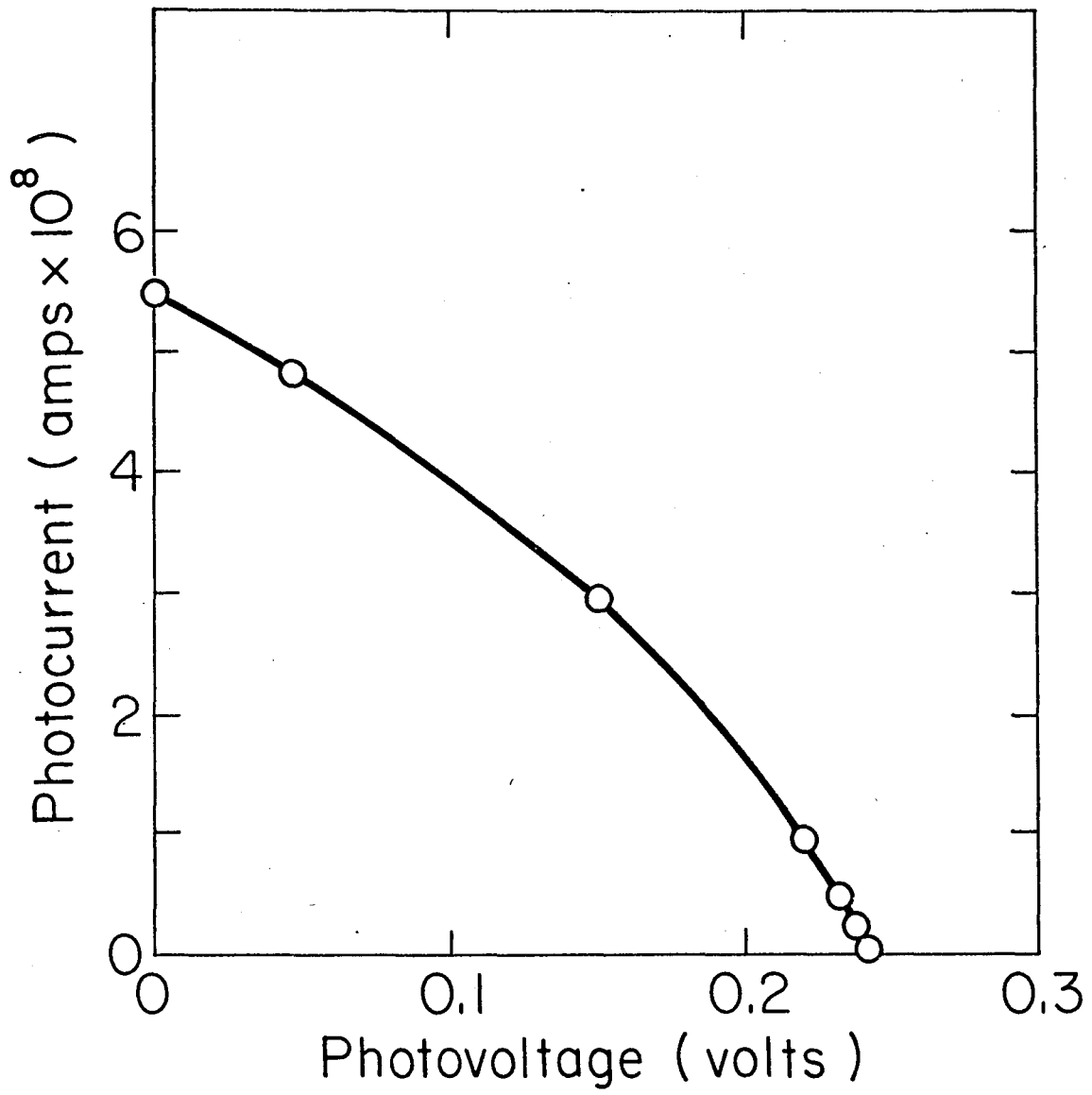


Fig. 3

XBL796-4885

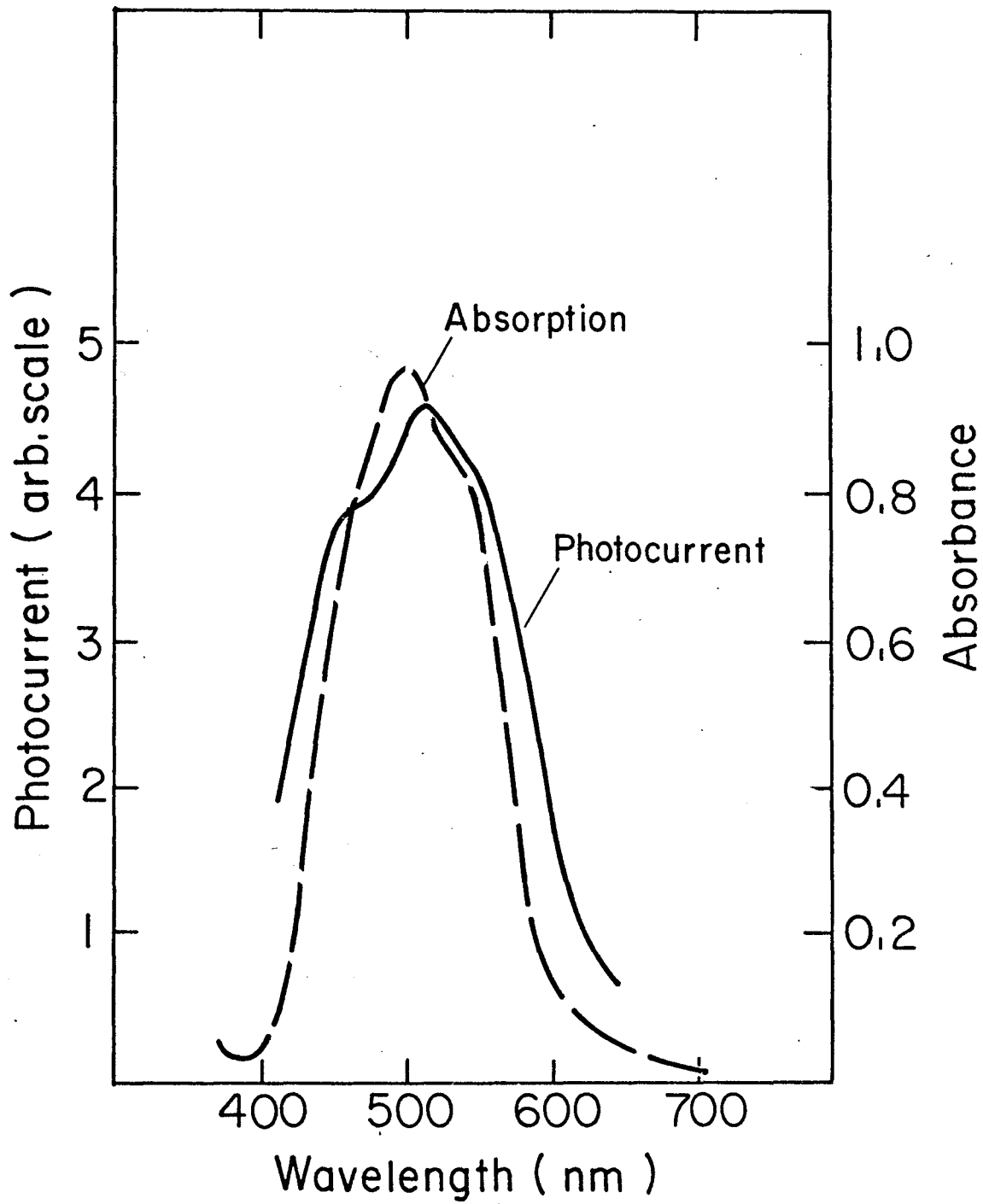


Fig. 4

XBL797-4899

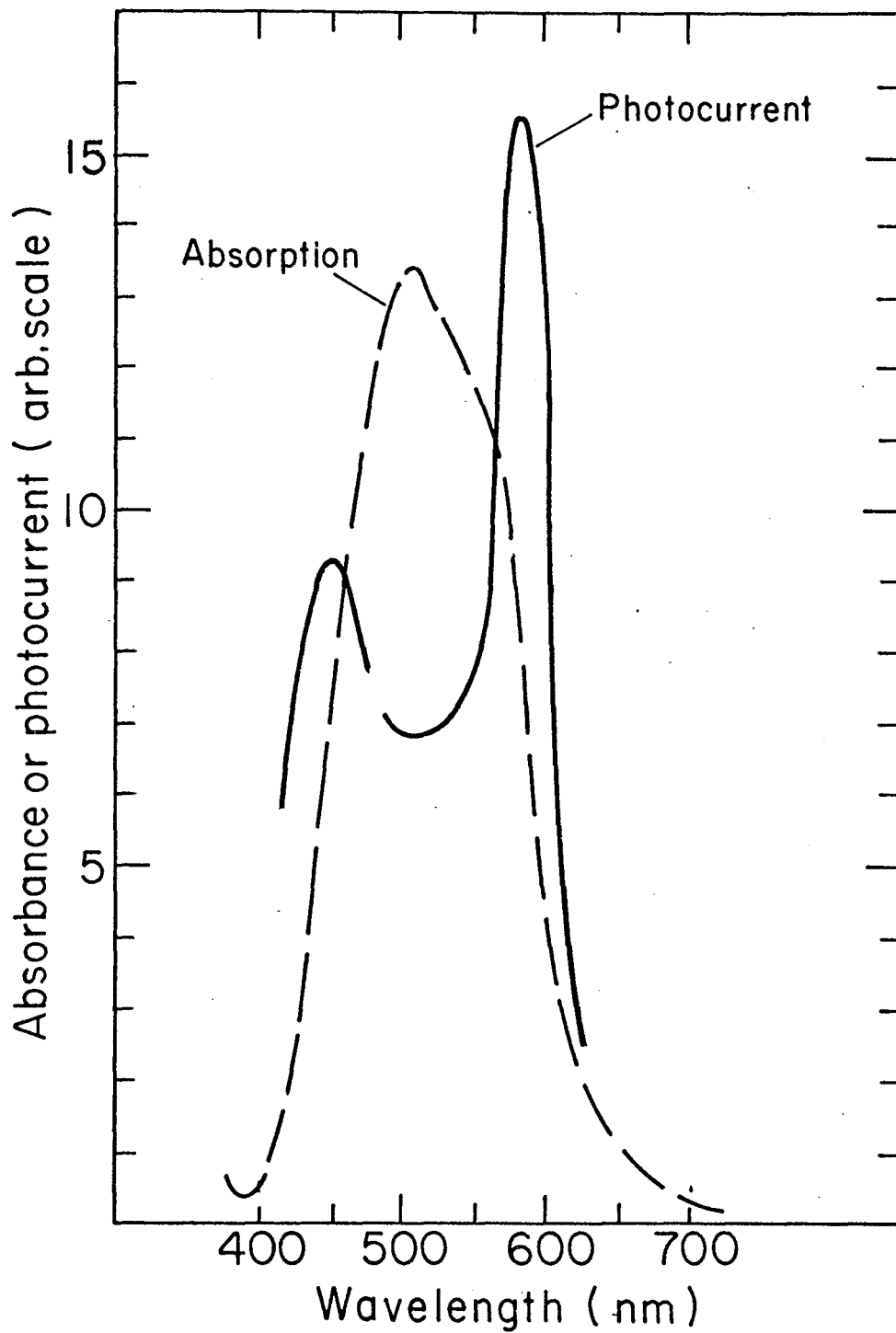


Fig. 5

XBL797-4892

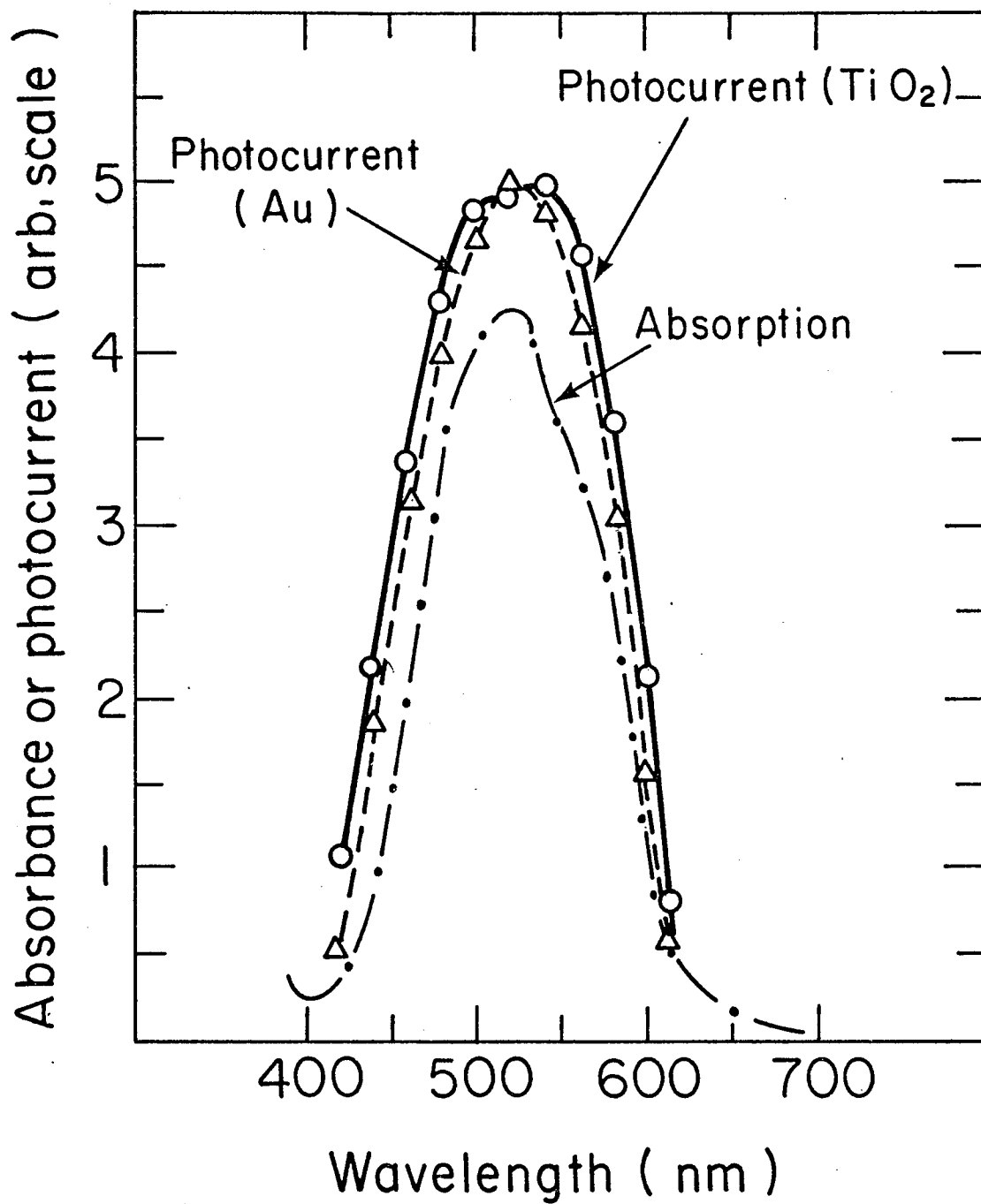


Fig. 6

XBL797-4893

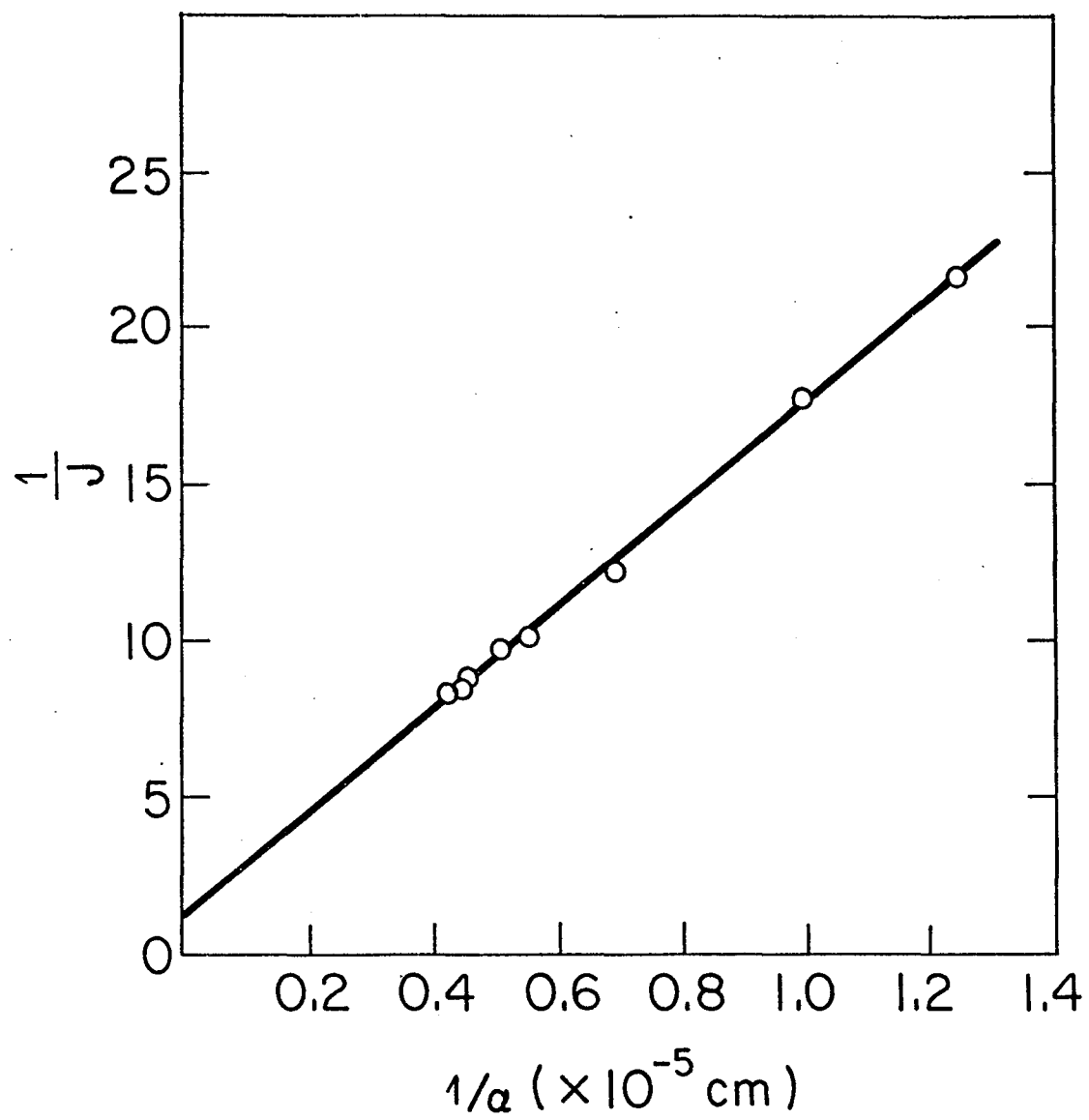


Fig. 7

XBL796-4847

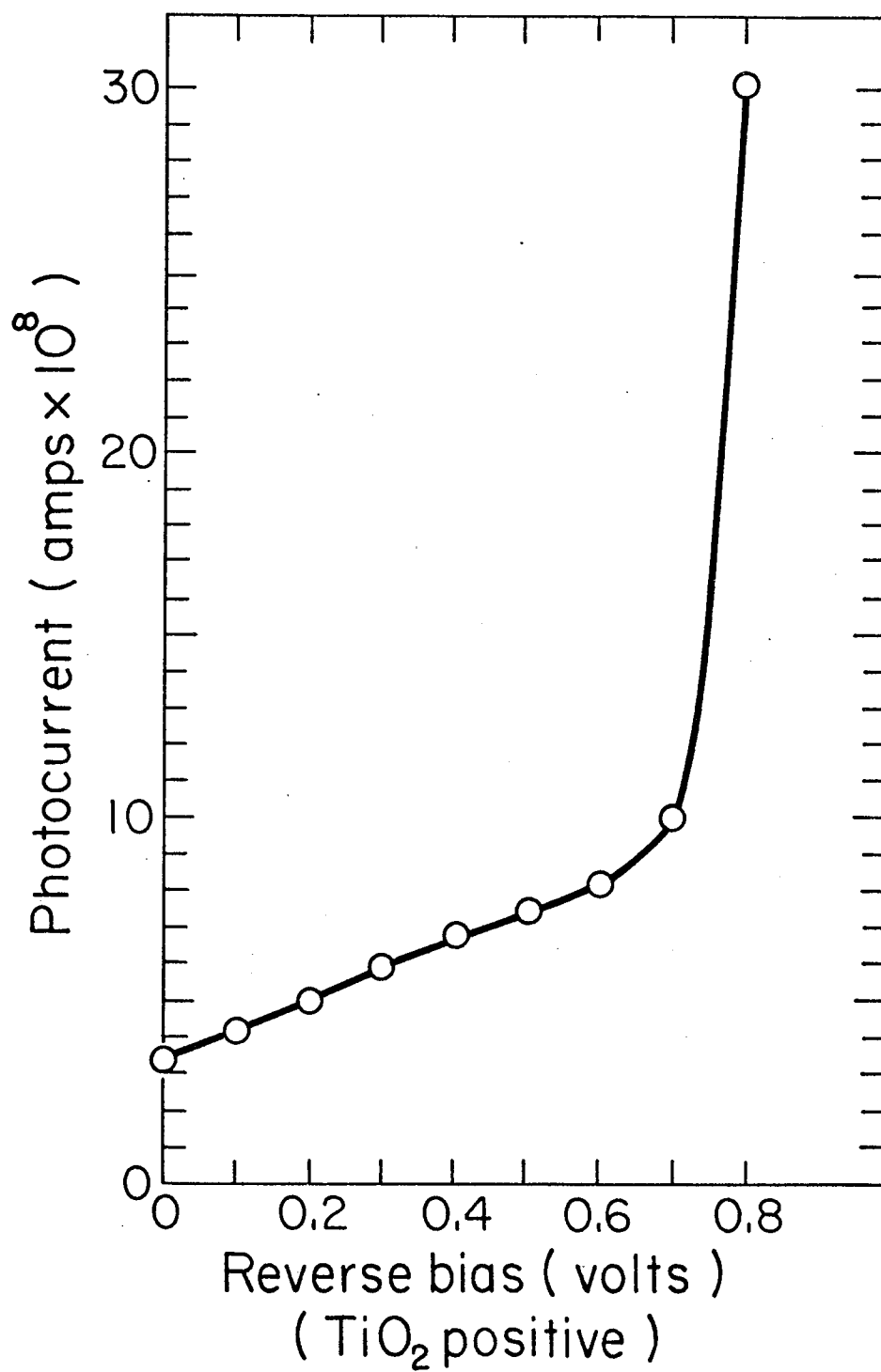


Fig. 8

XBL 797-4886

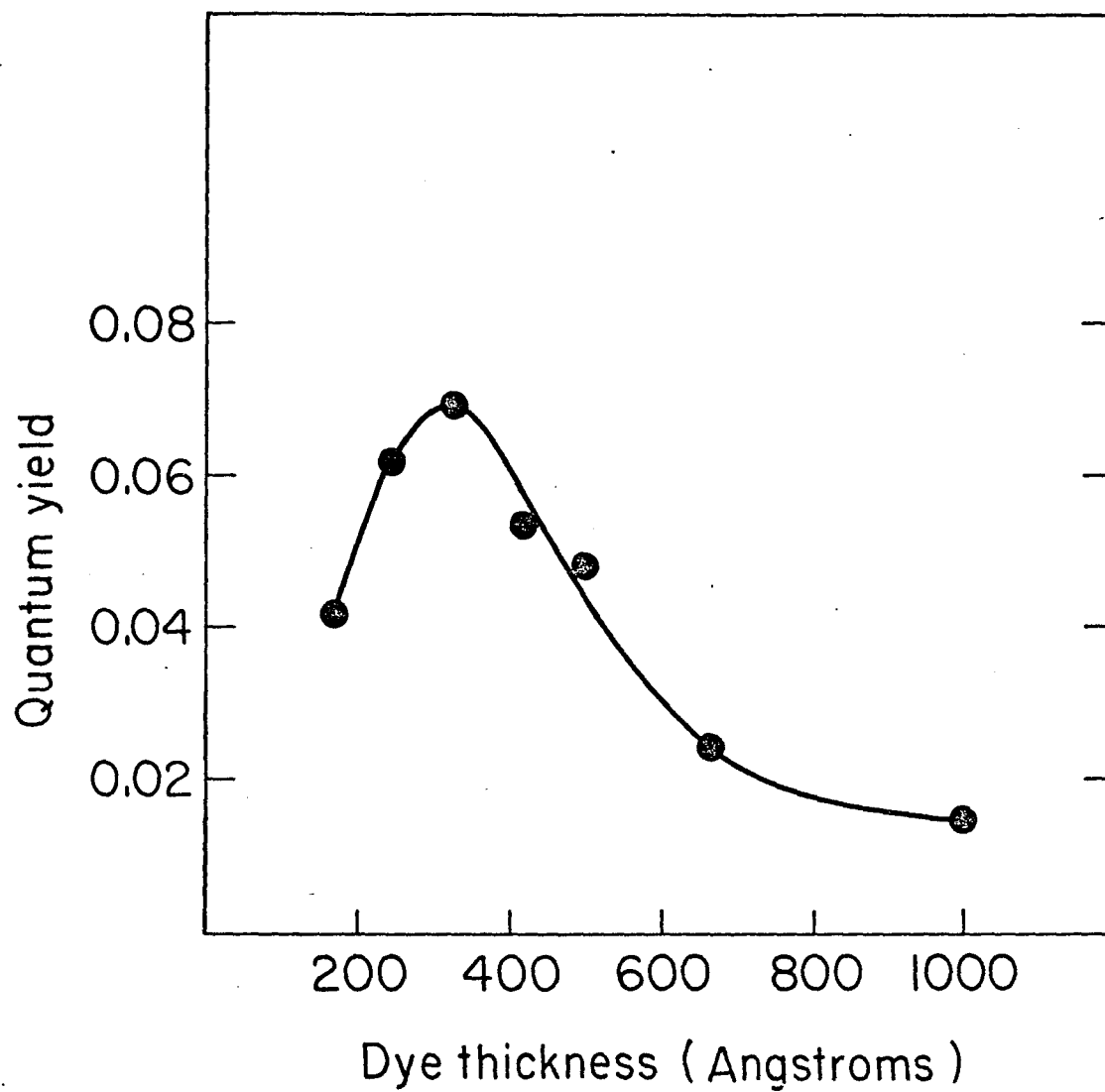


Fig. 9

XBL796-4836

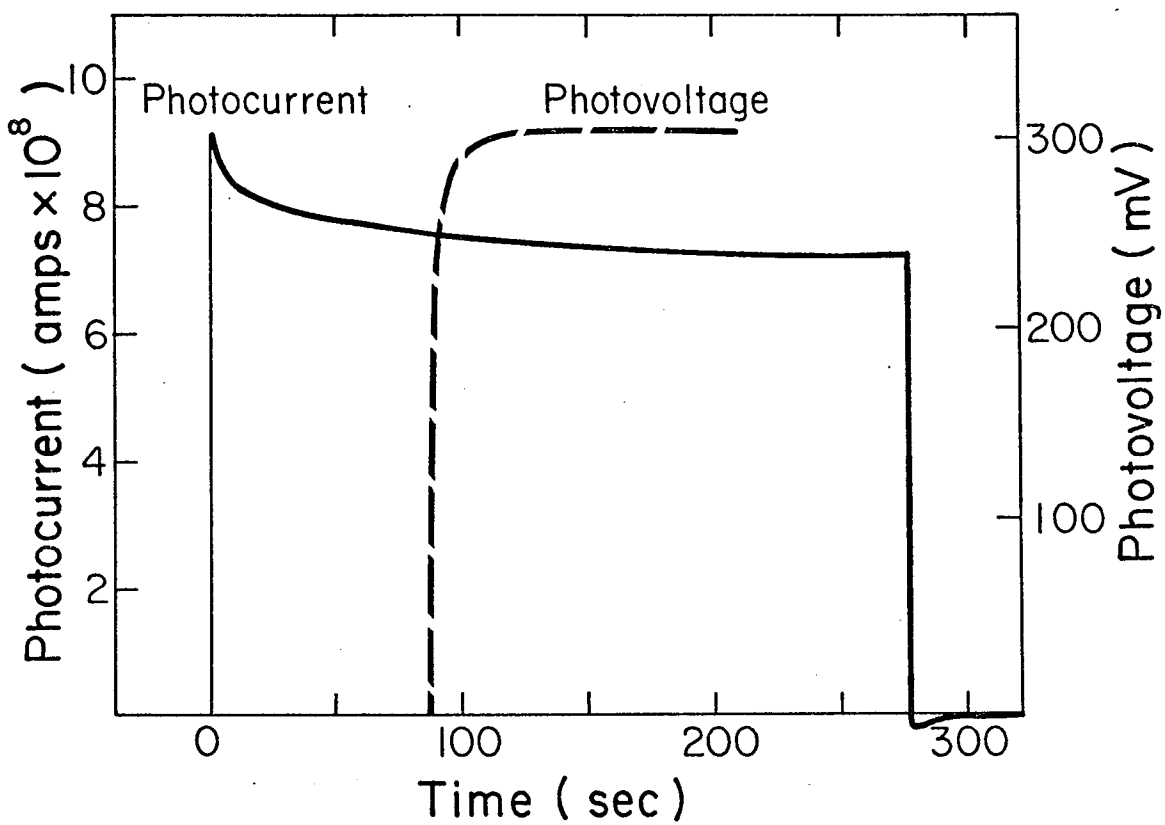


Fig. 10

XBL797-4901

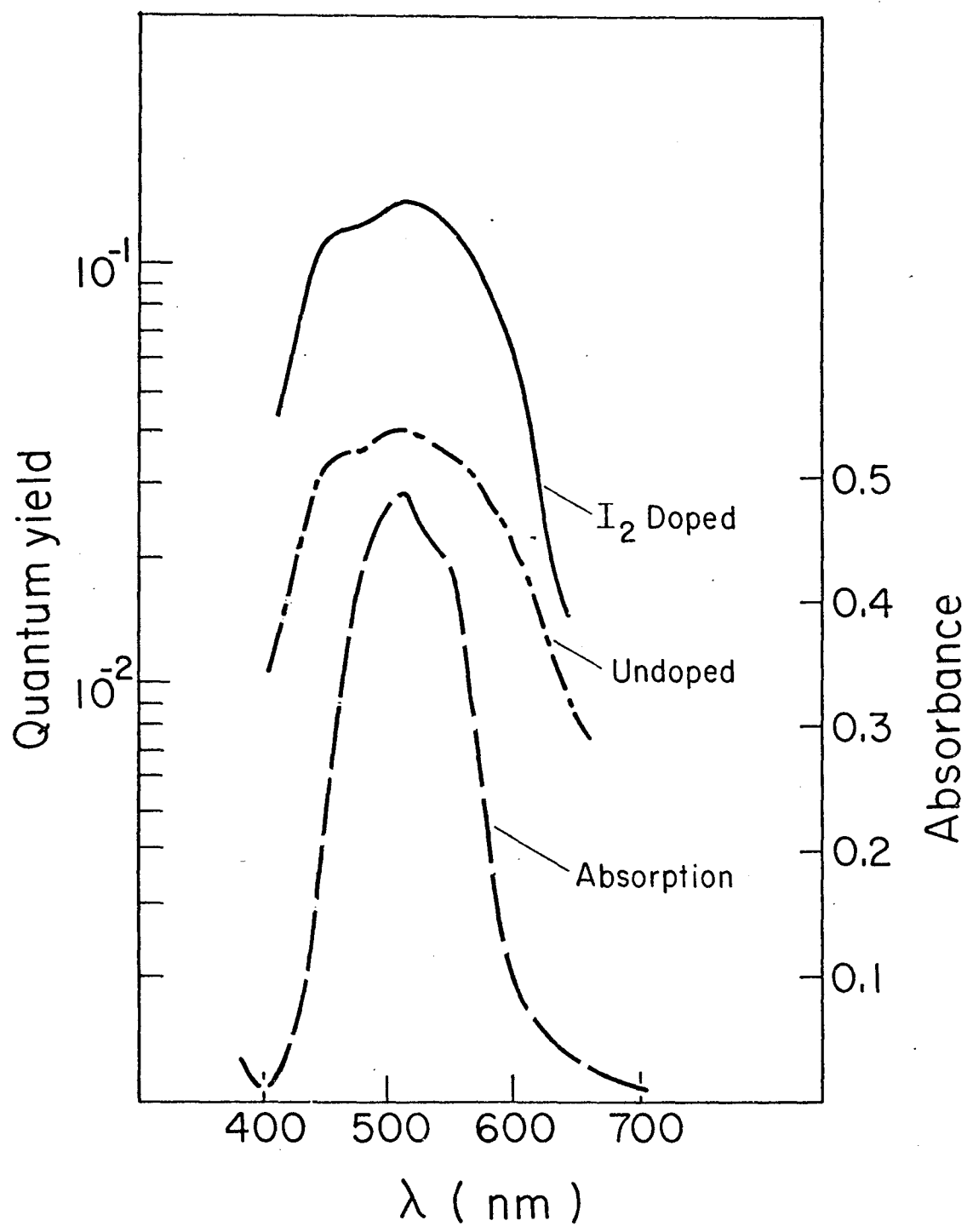


Fig. 11

XBL796-4840

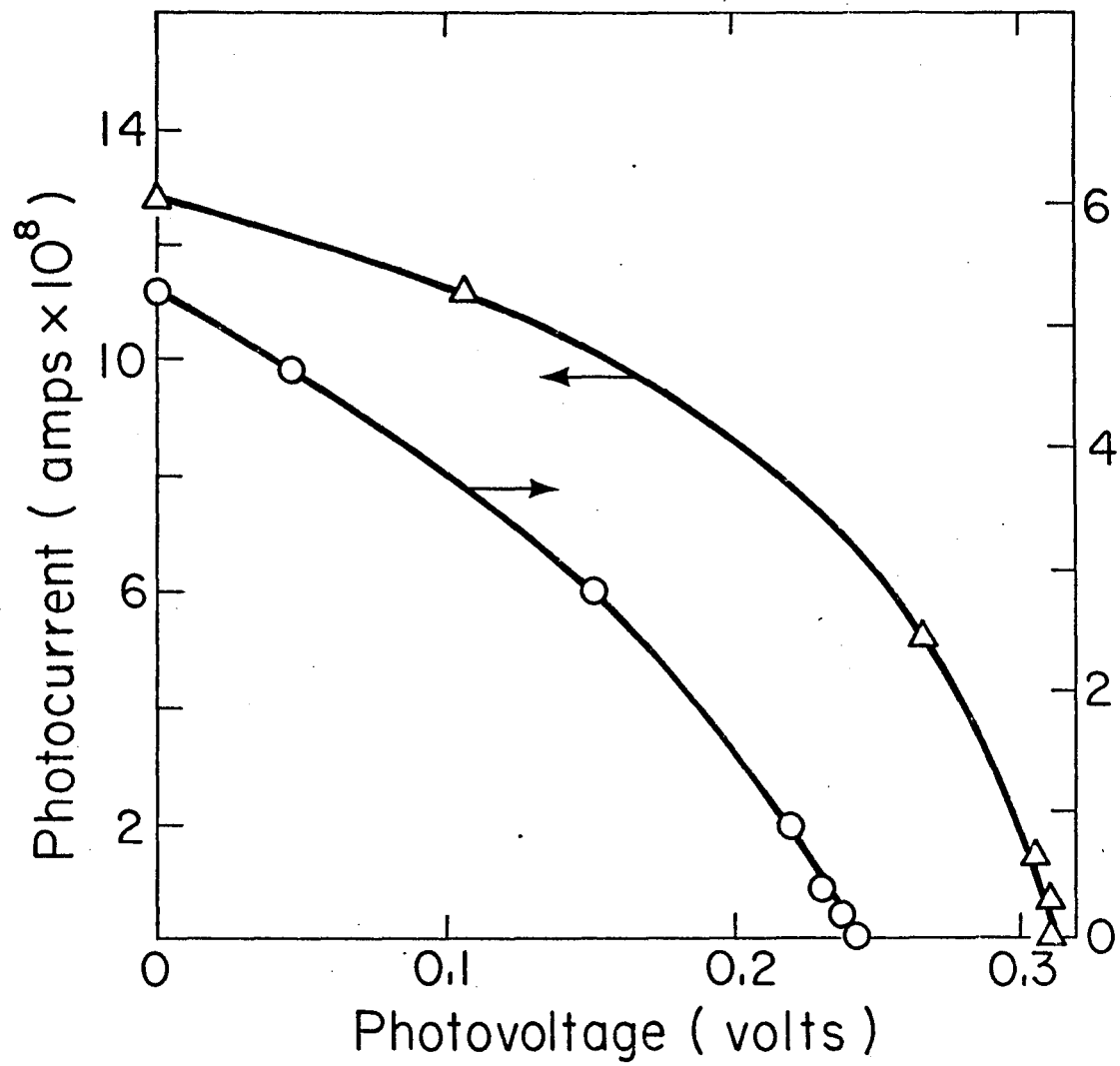


Fig. 12

XBL797-4884

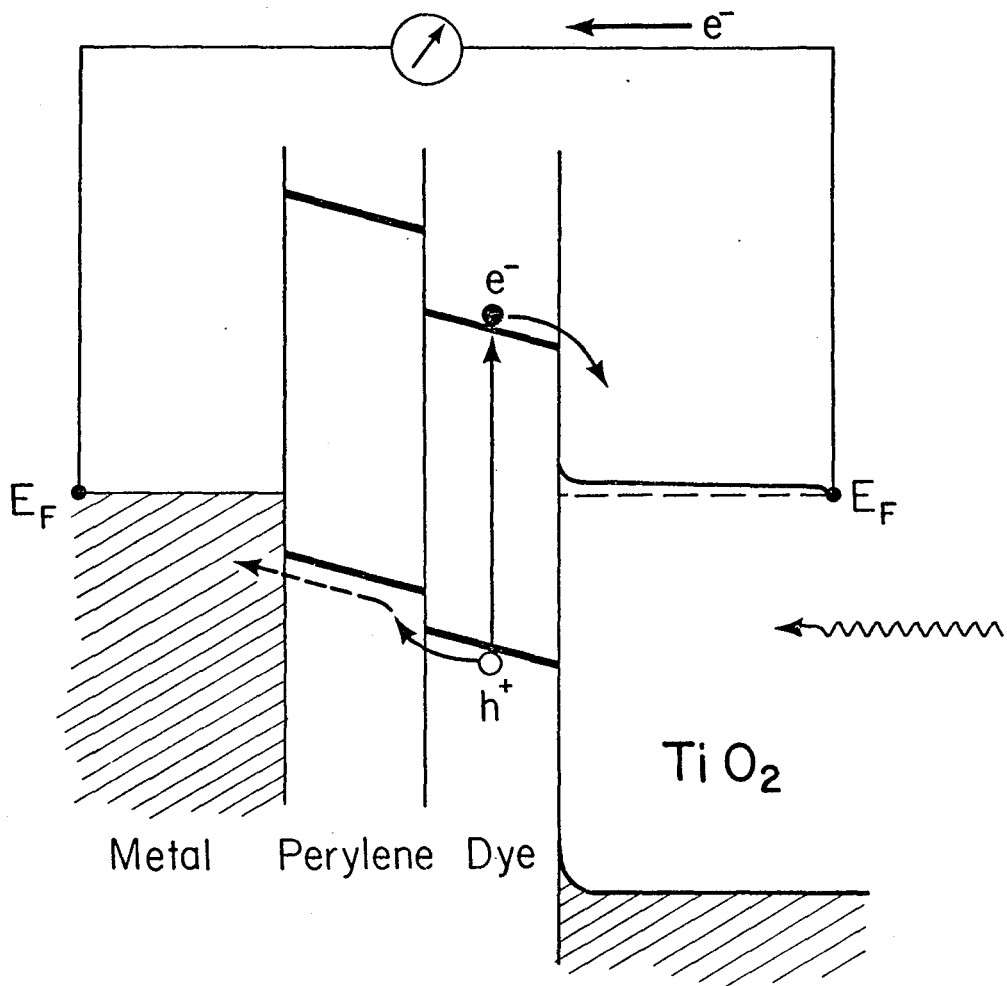


Fig. 13

XBL 796-4833

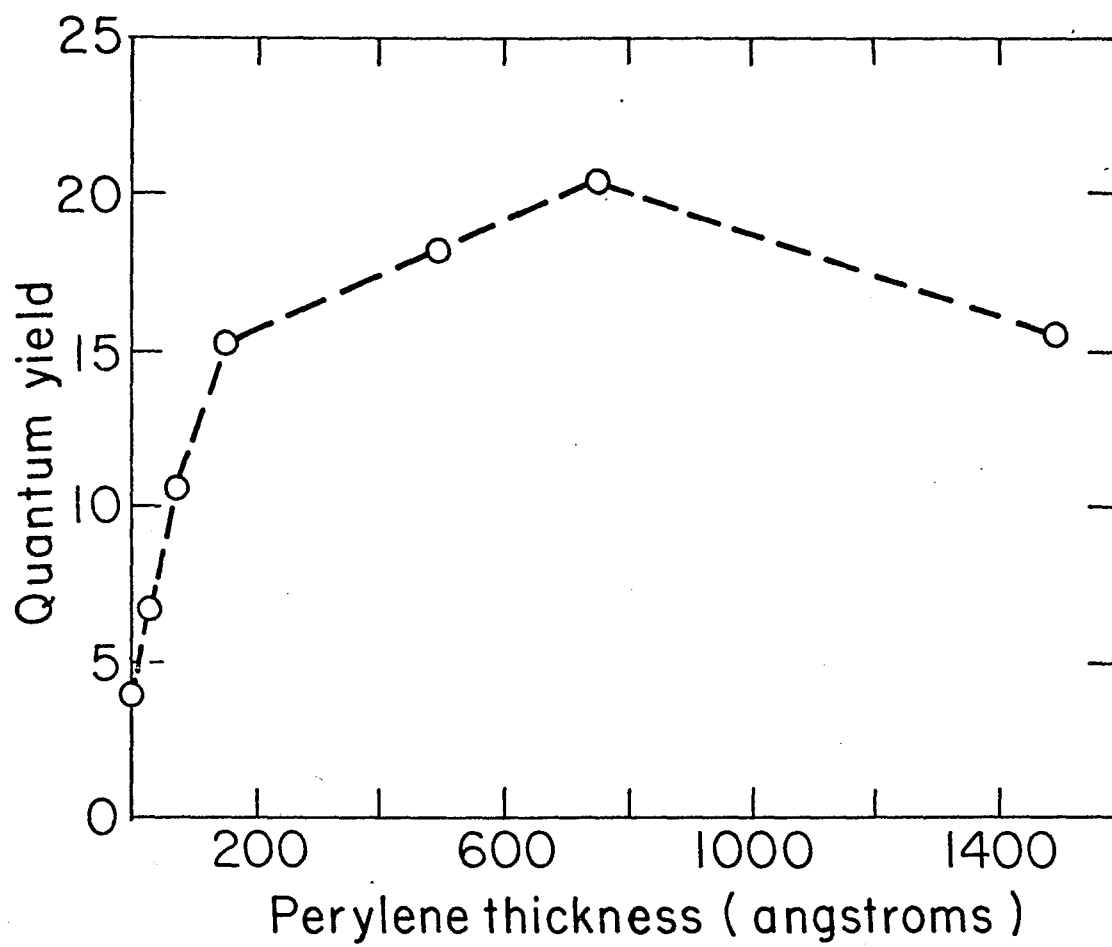


Fig. 14

XBL797-4895

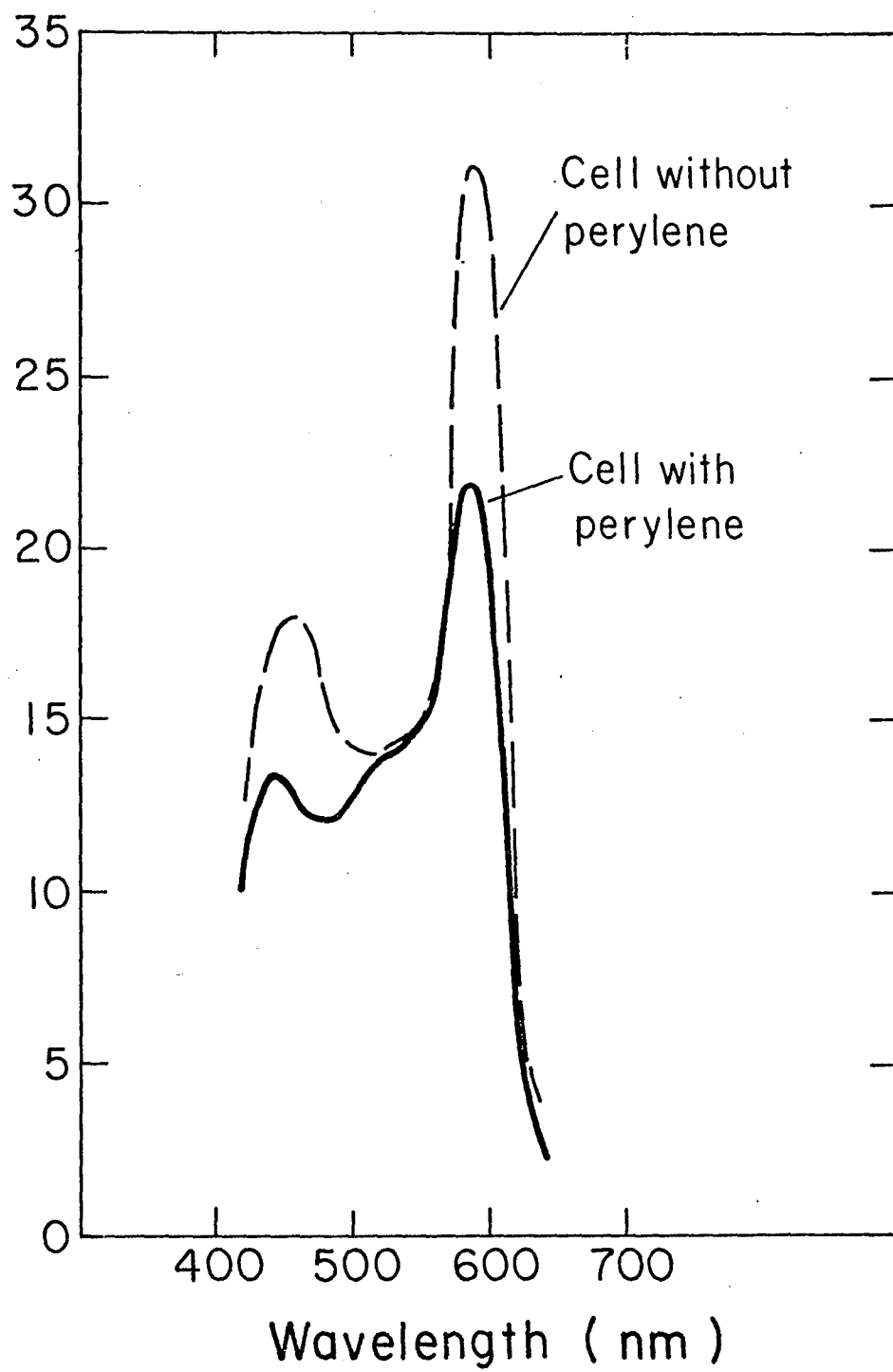


Fig. 15

XBL797-4904

This report was done with support from the United States Energy Research and Development Administration. Any conclusions or opinions expressed in this report represent solely those of the author(s) and not necessarily those of The Regents of the University of California, the Lawrence Berkeley Laboratory or the United States Energy Research and Development Administration.